Published in "Hydrological Processes 25 doi: 10.1002/hyp.8276, 2011"
which should be cited to refer to this work.

Runoff evolution in the Swiss Alps: projections for selected high-alpine catchments based on *ENSEMBLES* scenarios

Daniel Farinotti,[1]* Stephanie Usselmann,[1] Matthias Huss,[2] Andreas Bauder[1] and Martin Funk[1]

[1] *Laboratory of Hydraulics, Hydrology and Glaciology (VAW), ETH Zurich, CH-8092 Zurich, Switzerland*
[2] *Department of Geosciences, University of Fribourg, CH-1700 Fribourg, Switzerland*

Abstract:

The Alps are often referred to as the 'water tower of Europe'. In Switzerland, many branches of the economy, especially the hydropower industry, are closely linked to and dependent on the availability of water. Assessing the impact of climate change on streamflow runoff is, thus, of great interest. Major efforts have already been made in this respect, but the analyses often focus on individual catchments and are difficult to intercompare. In this article, we analysed nine high-alpine catchments spread over the Swiss Alps, selected for their relevance to a wide range of morphological characteristics. Runoff projections were carried out until the end of the current century by applying the *Glacier Evolution Runoff Model* (*GERM*) and climate scenarios generated in the framework of the *ENSEMBLES* project. We focused on assessing the uncertainty induced by the unknown climate evolution and provided general, statistically based statements, which should be useful as a 'rule of thumb' for analyses addressing questions related to water management. Catchments with a high degree of glacierization will undergo the largest changes. General statements about absolute variations in discharge are unreliable, but an overall pattern, with an initial phase of increased annual discharge, followed by a phase with decreasing discharge, is recognizable for all catchments with a significant degree of glacierization. In these catchments, a transition from glacial and glacio-nival regime types to nival will occur. The timing of maximal annual runoff is projected to occur before 2050 in all basins. The time of year with maximal daily discharges is expected to occur earlier at a rate of $4{\cdot}4 \pm 1{\cdot}7$ days per decade. Compared to its present level, the contribution of snow- and icemelt to annual discharge is projected to drop by 15 to 25% until the year 2100.

KEY WORDS runoff evolution; glacier hydrology; high-alpine basins; climate-change impact; *ENSEMBLES* scenarios

INTRODUCTION

Various ecosystems and millions of European citizens depend on rivers for their water availability (EEA, 2009). Many of the largest rivers of Central Europe, such as the Rhine, Po, Rhone and several tributaries of the Danube, originate in the Alps which are thus often referred to as the 'water tower of Europe' (e.g. Liniger and others, 1998; Viviroli and others, 2007). Many factors affect water management decisions—demography, global economy, societal values and norms, technological innovations and laws—but the primary driving factor of the water cycle is the climate. With the publication of the *Fourth Assessment Report* of the *Intergovernmental Panel on Climate Change* (IPCC, 2007), policymakers have accepted that the warming of the climate system is unequivocal. Accordingly, the efforts to assess future impacts have increased significantly in recent years. Many studies (e.g. Viviroli and others, 2007; Stahl and others, 2008; Steward, 2009; de Jong and others, 2009; Viviroli and others, 2011) have focused on mountain environments—the regions where water starts to merge into rivers and becomes manageable.

In Europe, the Alps represent the most important topographic feature affecting meteorological synoptic systems: large-scale phenomena are modified by the induced cyclogenetic processes (e.g. Mesinger and Pierrehumbert, 1986) and the development of mesoscale circulations (Wallén, 1970). Runoff generation in mountain regions is affected by these kinds of processes and is accordingly complex (Becker, 2005); therefore, making reliable projections is a challenge.

Switzerland is one of the European countries which looks at these projections with attention, as the Swiss economy, and especially the hydropower industry, is strongly dependent on the availability of water resources (Romerio, 2008a,b). Although a number of good reviews of the current understanding of climate-change impacts on Alpine regions exist (e.g. de Jong, 2005 Huber and others, 2005; Schädler and Weingartner, 2010; Viviroli and others, 2011), much of the information is spread over studies addressing only a few basins (e.g. Jasper and others, 2004; Gremaud and Goldscheider, 2010), often exploited for hydropower production (e.g. Schäfli and others, 2007; Huss and others, 2008b). Moreover, the non-uniformity of the input data used, the climate scenarios and the modelling approaches, make the intercomparison of the results difficult in many cases. Only a few examples of more comprehensive studies exist for

* Correspondence to: Daniel Farinotti, Laboratory of Hydraulics, Hydrology and Glaciology (VAW), ETH Zurich, CH-8092 Zurich, Switzerland.
E-mail: farinotti@vaw.baug.ethz.ch

the Swiss Alps (e.g. Horton and others, 2006), whereas larger efforts have been invested in the analysis of mesoscale catchments (e.g. Engelen, 2000; Ludwig and others, 2003; Hattermann and others, 2008; Mauser and Bach, 2009; Weber and others, 2010).

In this study, we assess the effect of climate change on the streamflow runoff of nine selected high-alpine catchments in the Swiss Alps. Our analyses emphasize the uncertainty induced by the projected climate evolution, using 10 different scenarios generated in the framework of the *ENSEMBLES* project—a European project led by the UK Met Office with the aim of 'allowing the uncertainty in climate projections to be measured' (van der Linden and Mitchell, 2009). For each catchment, we try to reconstruct the hydrological history since 1900 and force our conceptual, deterministic, glacio-hydrological model with 100 possible future meteorological time series. This allows a confidence band to be included in our projections. In the presentation of the results, we focus on highlighting hydrological features which are common to the different catchments and formulate statistically supported, general statements, which should be useful as a

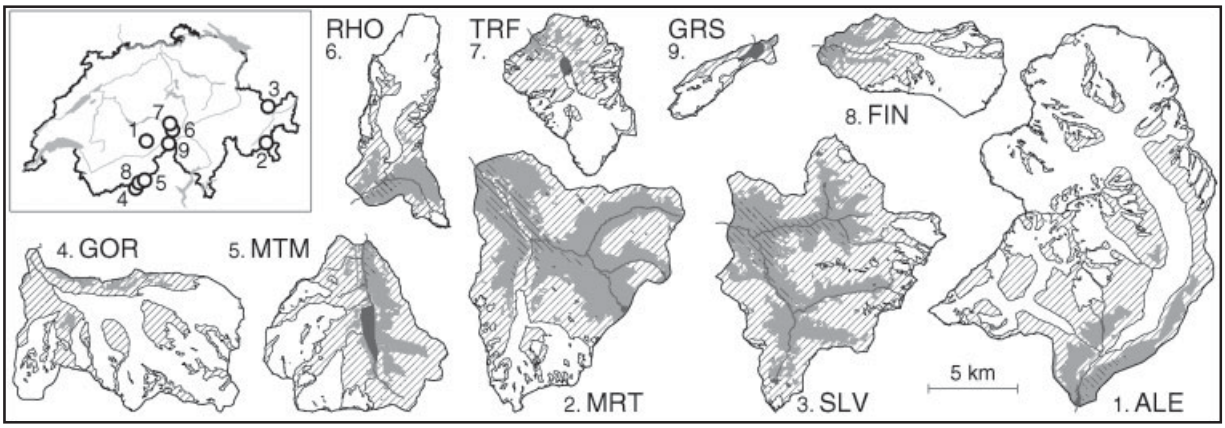

Figure 1. Overview of the analysed catchments. Abbreviations (ordered by catchment size): Aletsch (ALE), Morteratsch (MRT), Silvretta (SLV), Gorner (GOR), Mattmark (MTM), Rhone (RHO), Trift (TRF), Findel (FIN), Key for surface type designation is found in Figure 2

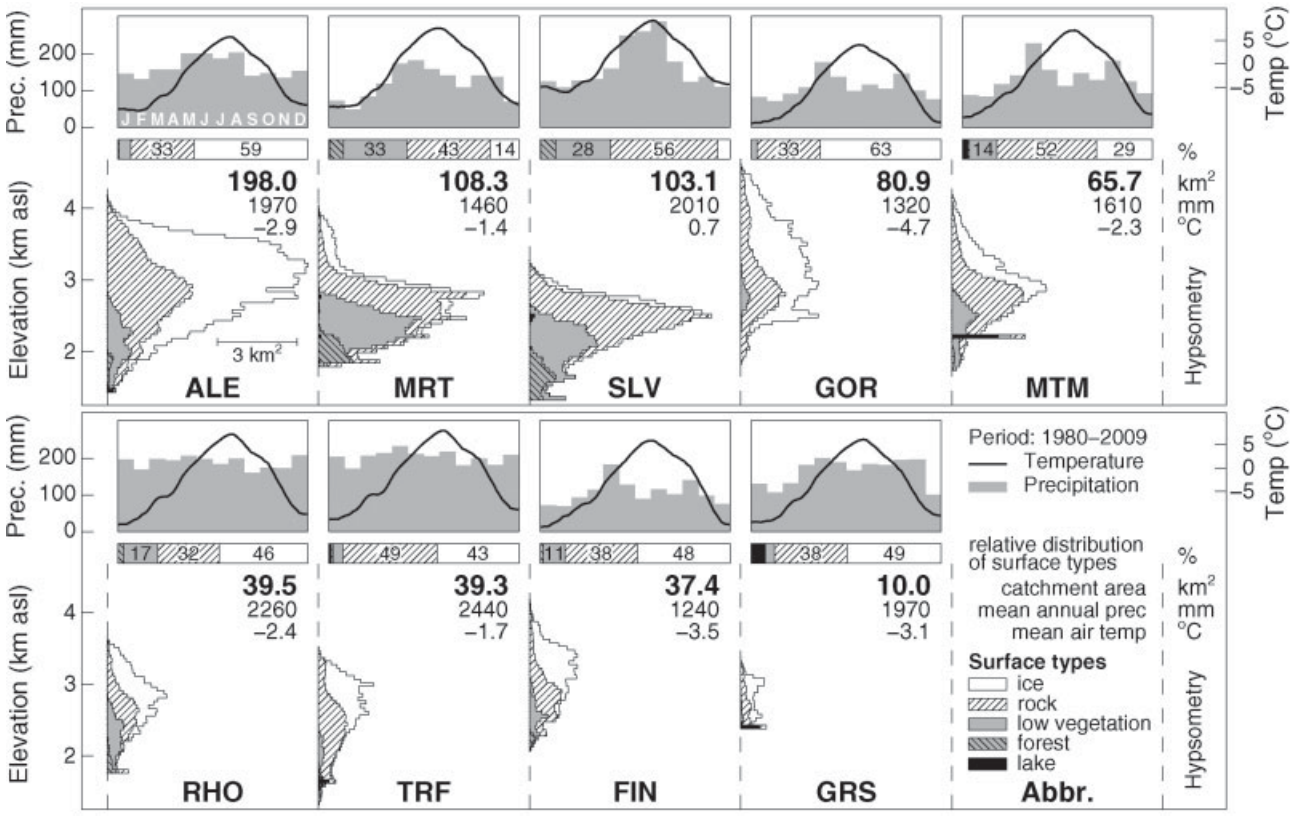

Figure 2. Morpho-climatological characteristics of the analysed catchments. The distribution with altitude (hypsometry) of the five surface types is shown. The relative distribution is shown in order to allow intercomparison between catchments. The mean annual course of temperature and precipitation is indicated for the reference period 1980–2009. Values correspond to means over the catchment. The catchment abbreviation key is found in Table I. Sequence corresponds to rank of catchment size. Surface types are designated according to the key in Figure 2

'rule of thumb' for questions linked to water management and water-supply safety in Alpine regions.

STUDY SITES AND DATA

In this study, we consider nine high-alpine catchments spread over the Swiss Alps (Figure 1) for which discharge data are available. The morpho-climatological characteristics of each catchment are summarized in Figure 2. The catchments are chosen in order to cover as many different conditions as possible: catchment size varies between 10 and 200 km^2, current glacierization between 7 and 63%, annual precipitation between 1300 and 2300 mm and exposure of the individual glaciers between north and south.

For each catchment, a variety of direct measurements are available. Data include repeated digital elevation models (DEMs) derived from either the digitization of topographic maps or from airborne photogrammetry (Bauder and others, 2007), summer and winter mass balance for the glacierized surfaces (Huss and others, 2010a) and discharge time series in daily or monthly resolution. The ice thickness distribution of the individual glaciers was determined following the approach presented in Farinotti and others (2009a,b) including radio-echo sounding measurements available for each glacier Farinotti (2010). Climatological data for the past—i.e. temperature and precipitation time series—are retrieved from the archives of the *Federal Office of Meteorology and Climatology (MeteoSwiss)*, and for future projections, we rely on the climate scenarios developed in the framework of the *ENSEMBLES* project (van der Linder and Mitchell, 2009).

Table I gives an overview of the data sets available for each catchment and introduces an abbreviation for each basin used throughout the article.

GLACIER EVOLUTION RUNOFF MODEL (*GERM*)

The broad range of elevation and the pronounced spatial variability of meteorological phenomena pose a real challenge to the hydrological modelling of high-alpine catchments. Models need to cope with a variety of processes which are in constant interplay and which are not fully understood in some cases (Becker, 2005). At high altitudes, snow and ice play a determinant role in the water cycle and have to be handled adequately.

Our model is an enhanced version of the *GERM* model presented by Huss and others (2008b), and consists of five different modules dealing with accumulation, ablation, glacier evolution, evapotranspiration and runoff routing, respectively. The model is a fully distributed, deterministic, conceptual model, designed for simulations at daily resolution, works on a 25×25 m grid and is forced with daily time series of temperature and precipitation. Six surface types are distinguished: ice, snow, rock, low vegetation (pasture), high vegetation (forest) and open water. The individual modules rely largely on existing approaches and are presented briefly hereafter.

Modules

Accumulation. At any grid cell i, accumulation—i.e. solid precipitation—$P_{\mathrm{sol},i}$ is computed by:

$$P_{\mathrm{sol},i} = P_{\mathrm{ref}} \cdot (1 + c_{\mathrm{prec}}) \cdot [1 + (z_i - z_{\mathrm{ref}}) \cdot \mathrm{d}P/\mathrm{d}z] \cdot D_{\mathrm{snow},i} \cdot r_{\mathrm{s}}, \quad (1)$$

Table I. Overview of data availability in each catchment

TLC	Name	Glaciers in catchment	DEMs	Discharge	Mass balance	
					Summer	Winter
ALE	Aletsch	Grosser Aletsch, Oberaletsch, Mittelaletsch	*1926 1957* 1999	1922–2007	1920–2009	1920–2009
MRT	Morteratsch	Morteratsch, Pers, Boval	*1936 1955* 1985 2008	1954–2008	1948–2008	1948–2008
SLV	Silvretta	Silvretta, Verstancla	*1938 1959 1973* 1986 1994 2003 2007	1933–2004	1917–2009	1914–2009
GOR	Gorner	Gorner, U. Theodul, Schwärze, Breithorn	*1931* 1982 2003 2007	1969–2007	2004–2007	2004–2007
MTM	Mattmark	Allalin, Hohlaub, Schwarzberg, Sewjinen, Chessjen	*1932 1946 1956 1967* 1982 1991 1999 2004, 2008	1998–2009	1955–2006	1955–1996
RHO	Rhone	Rhone, Tiertälli, Mutt	*1929* 1959 1980 1991 2000 2007	1900–2007[a]	1979–2009	1979–2009
TRF	Trift	Trift	*1929* 1980 1990 1995 2000 2003 2008	1997–2009	2002–2003	—
FIN	Findel	Findel, Adler	*1930* 1982 2007	1962–2008	—	—
GRS	Gries	Gries	*1923 1961 1967 1979* 1986 1991 1998 2003 2007	1957–2004[b]	1961–2009	1993–2009

'TLC' is the three-letter code used for abbreviation. The name of the most important glaciers included in the catchments are given (listed by glacier size). 'DEMs' list the years for which DEMs are available (in *italic* type: acquired from topographic maps; in roman type: acquired from airborne photogrammetry). 'Discharge' indicates the period for which daily discharge is available. For summer and winter mass balance, the year of the first and the last field survey is given. Catchments are listed in decreasing order of size.
[a] Gaps between 1904–1918 and 1929–1955.
[b] Only monthly data.

where P_{ref} is the precipitation at the reference location (in our study the centre of the basin), c_{prec} a correction factor which accounts for the gauge-catch deficit (Bruce and Clark, 1981), $z_i - z_{\mathrm{ref}}$ the elevation difference between the reference and the considered location, dP/dz the lapse rate with which precipitation increases with elevation (Peck and Brown, 1962), $D_{\mathrm{snow},i}$ a spatially distributed factor which accounts for snow redistribution processes (e.g. Tarboton and others, 1995; Huss and others, 2009) and r_{s} the fraction of solid precipitation. $D_{\mathrm{snow},i}$ is determined from characteristics of the surface topography (Huss and others, 2008a) and r_{s} decreases linearly from 1 to 0 in the temperature range $T_{\mathrm{thr}} - 1\,^{\circ}\mathrm{C}$ to $T_{\mathrm{thr}} + 1\,^{\circ}\mathrm{C}$, where T_{thr} is a threshold temperature distinguishing snow from rainfall (Hock, 1999). According to the definition of r_{s}, liquid precipitation at any grid cell i can be computed with Equation (1) by replacing r_{s} with $(1 - r_{\mathrm{s}})$ and setting $D_{\mathrm{snow},i}$ to 1.

Ablation. Ablation is modelled with a distributed temperature-index approach which includes the effect of solar radiation (Hock, 1999). The melt M_i at any grid cell i is calculated as:

$$M_i = (f_{\mathrm{M}} + r_{\mathrm{snow/ice}} \cdot I_{\mathrm{pot},i}) \cdot \overline{T}_i \quad \text{if } \overline{T}_i > 0\,^{\circ}\mathrm{C}, \qquad (2)$$

where f_{M} is a melt factor, $r_{\mathrm{snow/ice}}$ two distinct radiation factors for snow and ice, $I_{\mathrm{pot},i}$ the potential direct clear-sky solar radiation at the grid cell i and $\overline{T}_i$ the mean daily air temperature at the same location. For days with $\overline{T}_i \leq 0\,^{\circ}\mathrm{C}$, no melt occurs. The spatial distribution of $\overline{T}_i$ is obtained by interpolating the temperature at the reference location by means of a constant lapse rate. For exposed firn areas, melt is computed by setting the radiation factor to the average of snow and ice.

Glacier evolution. Glacier geometry is updated annually according to a non-parametric approach proposed by Huss and others (2010b). The updating is performed by redistributing the modelled annual change in mass according to a glacier-specific, elevation-dependent function Δh. The function is derived from the observed distribution of surface elevation change along the glacier (Huss and others, 2010b). The Δh-approach is mass-conserving and prescribes the most pronounced changes happening in the tongue region. Geometry changes in the accumulation zone are minor. The performance of the approach and its suitability for applications in climate change impact studies was addressed in detail in Huss and others (2010b) who compared the results of the Δ h-approach with those obtained with a 3D finite-element ice flow model (Jouvet and others, 2008).

Evapotranspiration. Actual evapotranspiration $ET_{\mathrm{act},i}$ at any grid cell i is computed by reducing the potential evapotranspiration calculated according to Hamon (1961) by a constant, surface-type depending factor $f_{\mathrm{ETp},j}$:

$$ET_{\mathrm{act},i} = \frac{35{\cdot}77 \cdot DL \times e_{\mathrm{s}}}{\overline{T}_i + 273{\cdot}3} \cdot S_j \cdot f_{\mathrm{ETp},j}. \qquad (3)$$

DL is the potential fraction of daylight per day (a function of the day of the year), e_{s} the saturation vapour pressure (a function of $\overline{T}_i$), $\overline{T}_i$ the mean daily air temperature (°C) at grid cell i and S_j an empirical factor characterizing the properties of surface-type j. Over ice surfaces, S_j can be negative, meaning that condensation occurs (e.g. Lang and others, 1977; Bernath, 1991). $f_{\mathrm{ETp},j}$ is set to 1 until an interception reservoir is not empty. The surface type j is a function of grid cell i.

Runoff routing. The runoff routing module is a further development of the scheme proposed in Huss and others (2008b). The module is based on the concept of linear reservoirs (e.g. Langbein, 1958) and distinguishes five surface types: ice, snow, rock, low vegetation (pasture), high vegetation (forest) and open water. The module solves the local water balance

$$Q_i = P_{\mathrm{liq},i} + M_i - ET_i - \sum_r \Delta V_{r,i} \qquad (4)$$

at all grid cells for every time step, Q_i being the runoff and $\Delta V_{r,i}$ the storage change of reservoir r. Figure 3 is a schematic illustration of the module.

When a given grid cell is snow-free, three reservoirs, named hereafter *interception*, *fast* and *slow* reservoir, are active. The interception reservoir represents the intercepted precipitation, has a limited, surface-type-dependent capacity $V_{\mathrm{int\_max},j(i)}$ and is filled first at every event of liquid precipitation (in the notation, the subscript $j(i)$ indicates that the surface type j is a function of the considered grid cell i). If the amount of liquid precipitation occurring at any location is larger than $V_{\mathrm{int\_max},j(i)}$, the slow reservoir, representing subsurface

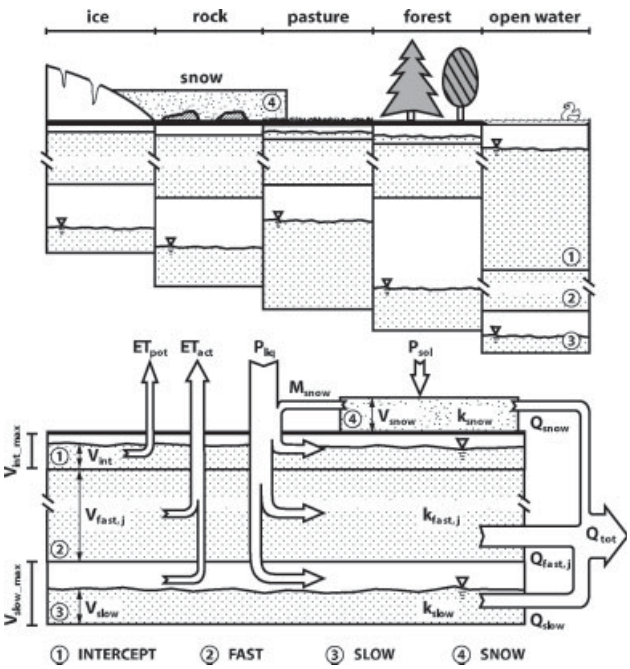

Figure 3. General scheme of the runoff routing module. The upper scheme illustrates the way different surface types (ice, rock, pasture, forest and open water) are represented. The lower scheme applies to each surface type and shows how the different reservoirs (intercept, fast, slow and snow) are linked to the components of the water balance. Parameters are shown as in the text

runoff components, is filled. The volume ${}^{+}\Delta V_{\mathrm{slow},i}$ added to the slow reservoir is dependent on its filling level $V_{\mathrm{slow},i}$ (Schäfli and others, 2005):

$$ {}^{+}\Delta\ V_{\mathrm{slow},i} = (P_{\mathrm{liq},i} + M_i) \cdot \left(1 - \left(\frac{V_{\mathrm{slow},i}}{V_{\mathrm{slow\_max},j(i)}}\right)^2\right), \qquad (5) $$

where $V_{\mathrm{slow\_max},j(i)}$ is the surface-type dependent capacity of the slow reservoir and M_i the melt computed according to Equation (2). To reduce the degrees of freedom of the model, the relative size of $V_{\mathrm{slow\_max},j(i)}$ is kept constant between surface types. By doing so, only a scaling factor f_{V} needs to be adjusted (Tables III and IV). The fraction of liquid precipitation not entering the slow reservoir, i.e. $(P_{\mathrm{liq},i} + M_i) - {}^{+}\Delta\ V_{\mathrm{slow},i}$, is added to the fast one, representing direct and near-surface runoff components. The capacity of the fast reservoir is potentially unlimited.

Solid precipitation is treated separately and builds up a snow cover. Once the snow cover is melting, a fourth reservoir (*snow* reservoir) becomes active and is filled. Its capacity is not limited.

The interception reservoir does not contribute to runoff and is emptied at the rate of potential evapotranspiration (potential ET). Whenever the filling level of the interception reservoir is insufficient for providing the whole computed potential ET, the difference is reduced to actual ET with the surface-type dependent factor $f_{\mathrm{ETp},j}$ and subtracted from the fast reservoir. If the entire amount cannot be provided by this reservoir, the remaining portion is taken from the slow reservoir. In the case where the slow reservoir becomes empty, ET is reduced to the maximal available amount.

The snow, fast and slow reservoirs are emptied by means of a reservoir-dependent retention constant k_r ($r =$ snow, fast or slow). For the fast reservoir, k_r is surface-type dependent. The contribution of grid cell i to discharge, i.e. Q_i, is then computed as:

$$ Q_i = \sum_r V_{r,i}/k_r, \qquad (6) $$

where $V_{r,i}$ is the filling level of reservoir r at grid cell i.

Open water surfaces are represented by grid cells with very large $V_{\mathrm{int\_max},i}$, small $V_{\mathrm{slow\_max},i}$ and the prescribed k_{fast}. This corresponds to storing water in the cells and evaporating it with the potential ET rate until the cell overspills.

The total discharge from the catchment is finally computed by adding Q_i for all grid cells inside the catchment.

Calibration

The accumulation and ablation modules are calibrated according to the iterative calibration scheme described in Huss and others (2008a). The scheme adjusts accumulation and melt parameters—i.e. c_{prec}, $\mathrm{d}P/\mathrm{d}z$, f_{M}, $r_{\mathrm{ice/snow}}$—in order to match direct measurements of winter mass balance (where available) and glacier ice volume change. Ice volume changes are derived from differencing two subsequent DEMs (Bauder and others, 2007). Local temperature lapse rates are obtained by linear regression from temperature records of the *MeteoSwiss* network. For each catchment, stations within a radius of 50 km were considered. The function necessary for the glacier geometry module is derived from the available DEMs (Huss and others, 2010b). Since no direct measurements are available for calibrating the evapotranspiration module, parameters are adjusted in order to match yearly evapotranspiration rates reported in the literature (e.g. Bernath, 1991; Verbunt and others, 2003).

The parameters of the runoff routing module are adjusted in order to maximize the agreement between calculated and measured discharge. Agreement is evaluated by considering daily, monthly and annual discharge, as well as by comparing the modelled and observed distribution of runoff during the year. The error induced by neglecting runoff concentration times in the model is considered of minor importance even at the daily time scale. In fact, in view of the morphology of each catchment and the approach by Kirpich (1940), one can expect concentration times smaller than a quarter of a day. Figure 4 shows scatter plots of measured *versus* simulated runoff and Table II states the Nash–Sutcliffe efficiencies (Nash and Sutcliffe, 1970) for the individual catchments. Aside

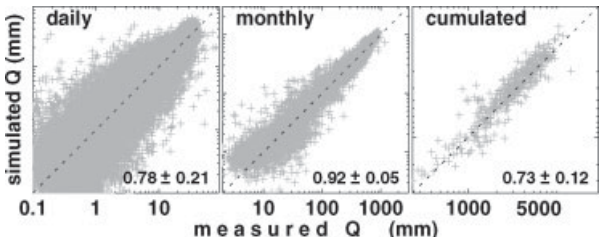

Figure 4. Scatter plots of measured *versus* simulated runoff (log-scale). The dotted line corresponds to a 1 : 1 relation. All catchments are displayed together. 'Cumulated' values are sums over the runoff measured during a one-year period. Since data are not available during the winter months for GOR and FIN, the aggregated values do not necessarily correspond to a sum over 365 days. The mean Nash-Sutcliffe efficiency over the nine catchments $\pm 1{\cdot}96\ \sigma$ is given in the lower-right corner

Table II. Nash–Sutcliffe efficiency for the individual catchments

	Nash-Sutcliffe efficiency		
Basin	Daily	Monthly	Cumulated
ALE	0·90	0·96	0·81
MRT	0·61	0·90	0·62
SLV	0·83	0·92	0·78
GOR	0·72	0·91	0·72
MTM	0·67	0·90	0·70
RHO	0·88	0·94	0·76
TRF	0·88	0·95	0·79
FIN	0·77	0·89	0·67
GRS	—	0·94	0·75

The criterion is computed during the whole period with measured runoff for daily, monthly and cumulated data. See Figure 4 for the definition of 'cumulated'.

Table III. Calibrated catchment-specific parameters

Parameter	Units	Catchment								
		ALE	MRT	SLV	GOR	MTM	RHO	TRF	FIN	GRS
f_M	10^{-3} m (d °C)$^{-1}$	1·349	1·211	1·032	0·931	1·069	1·316	1·212	1·001	1·447
r_{ice}	10^{-5} m^3 (W d °C)$^{-1}$	2·158	1·937	1·651	1·490	1·711	2·107	1·939	1·601	2·314
r_{snow}	10^{-5} m^3 (W d °C)$^{-1}$	1·618	1·452	1·238	1·118	1·284	1·579	1·454	1·200	1·735
dT/dz	10^{-3} °C m^{-1}	−5·65	−5·57	−5·47	−5·77	−5·86	−5·55	−5·45	−5·81	−5·47
dP/dz	10^{-2}% m^{-1}	5	5	0	2	0	7	5	7	1
c_{prec}	%	10	40	90	25	20	40	70	10	25
f_V	—	6	2	3	7	4	5	6	6	11

f_M, melt factor; $r_{ice/snow}$, radiation factor for ice and snow respectively; dT/dz, temperature lapse rate; dP/dz, precipitation lapse rate; c_{prec}, precipitation correction factor; f_V, scaling factor for V_{slow_max} (see Table IV).

Table IV. Calibrated surface-type specific parameters

Parameter	Units	Surface type					
		Ice	Snow	Rock	Pasture	Forest	Open water
V_{int_max}	mm	0·0	0·0	0·5	1·0	2·5	0·0
V_{slow_max}/f_V	mm	20	—	30	80	150	500
k_{fast}	d	2	5	4	9	15	30
k_{slow}	d	120	120	120	120	120	120
S	mm d^{-1}	−0·2	1·0	1·0	1·9	3·0	10·0
f_{ETp}	—	1·0	1·0	0·2	0·5	0·5	1·0

V_{int_max}, maximal capacity of the interception reservoir; V_{slow_max}, maximal capacity of the slow reservoir; k_{fast}, retention constant of the fast reservoir; S, empirical ET factor; f_{ETp}, reduction factor for potential ET. The retention constant for the slow reservoir k_{slow} is listed in the Table for convenience, although not surface-type dependent. Values for the scaling factor f_V are stated in Table III.

from SLV, a tendency in the efficiencies is recognizable, indicating that the model performs slightly less well for catchments with a lower degree of glacierization (i.e. MTM and MRT). This may be an indication that outside glacierized areas some relevant process, such as groundwater storage and flow or evapotranspiration, may not be represented adequately in the model.

The parameters of each module were assumed to be constant over time. The compilations of the parameters calibrated for each individual catchment are shown in Tables III and IV.

METEOROLOGICAL TIME SERIES

GERM requires continuous temperature and precipitation time series as input. Since none of the catchments has a local station that is available for the whole period 1900–2010, a meteorological time series with daily resolution has to be reconstructed. This is done by following the scheme presented in Huss and others (2008a) which treats temperature and precipitation separately. The temperature time series is generated by superposing the daily fluctuations recorded at the nearest weather station with continuous data since 1900 on a time series of monthly mean temperature reconstructed for the basin through an inverse-distance interpolation of homogenized time series available for 12 different *MeteoSwiss* stations (Begert and others, 2005). In contrast, the precipitation time series is generated by scaling the records of the closest weather station in order to match the monthly mean precipitation sums stated for the basin in the *PRISM* data set (Schwarb and others, 2001). The *PRISM* data set provides the spatial distribution of monthly precipitation sums during the period 1971–1990 for the Alpine region on a grid of about 2 km.

For simulations until the year 2100, time series of temperature and precipitation are required for the future as well. As in any study assessing the impact of climate change, the assumed climate evolution is central. In this contribution, we rely on climate scenarios developed in the framework of the European *ENSEMBLES* project (van der Linden and Mitchell, 2009). The project aimed at providing a range of projections for future climate evolution including probabilistic information, i.e. assessed to decide which of the outcomes are more likely (probable). This goal was achieved by following the concept of 'multiple model runs', a method known to improve the accuracy and reliability of forecasts. In the project, each run consisted of a 'model chain', i.e. a particular combination of a general circulation model (GCM) with a regional climate model (RCM).

In our study, we consider changes in temperature and precipitation as projected by 10 different model chains which all assume the SRES A1B emission scenario (IPCC, 2000). The data are provided by the *Center for Climate Systems Modeling (C2SM)* at ETH Zurich and are based on the 'delta change approach'. This approach expresses the effects of climate change between two

periods in terms of expected difference ('delta') in the mean of a given variable. The two periods have the same length (usually 30 years) and are called 'reference' and 'scenario period', respectively. Deltas do not need to refer to the annual mean, but can have finer resolution. For the location of each *MeteoSwiss station*, *C2SM* provides two sets of deltas in daily resolution (meaning that each day of the year has an individual delta, Bosshard and others, 2011). Both sets have the period 1980–2009 as reference, but have two different scenario periods, i.e. 2021–2050 and 2070–2099.

Modelling the hydrological response of high-alpine catchments to climate change requires transient simulations of the relevant processes—especially glacier retreat. In order to obtain transient scenarios from the deltas described above, a linear interpolation is performed between the periods, assuming that the stated delta applies exactly for the centre of the period. If we denote the mean of the variable X during the 30-year period $[t-15,\ t+14]$ with $\overline{X}(t)$ and the delta change between the reference period $[r-15,\ r+14]$ and the scenario period $[s-15,\ s+14]$ with $\Delta_{\mathrm{r-s}}$, we can write:

$$\overline{X}(t) = \overline{X}(r) + \frac{\Delta_{\mathrm{r-s}}}{s-r} \cdot t. \qquad (7)$$

Note that the equation applies individually for each day of the year since deltas are in daily resolution, and that in the case of precipitation, one needs to replace '+' with '×', as deltas are multiplicative in this case. Following this approach, the deltas in the 10 different model chains prescribe 10 possible evolutions of mean temperature and precipitation during the period 2010–2100. However, by doing so, one neglects the intrinsic year-to-year variability of the meteorological variables. In order to take into account this variability as well, we generate 10 different meteorological time series for each of the 10 prescribed evolutions of the mean. This is done by repeating the following procedure for each year in the future for which a meteorological time series is required: (1) randomly select a year in the past, (2) compute the daily deviations from the local, 30-year average, (3) add the interpolated, daily delta change signal to the daily values thus obtained. The final result is a set of 100 possible realizations of mean daily air temperature and daily precipitation sum for the period 2010–2100. For future projections, we run our model with each of the 100 generated meteorological time series. This gives the possibility to assess the bandwidth spanned by the underlying emission scenario and the climate models used.

For each catchment, the relevant time series of deltas was chosen by a nearest neighbour procedure, considering the centre point of the catchment and all *MeteoSwiss* stations. On average, the 10 scenarios predict an increase in mean annual temperature at a rate of +0·4 °C per decade (Figure 5A). This is consistent with the previous reference study for the Swiss Alps carried out by Frei (2007), who presented a statistical analysis of the simulations generated within the *PRUDENCE* project (Christensen and others, 2002; Christensen and Christensen, 2007). This is surprising to some degree, as the 16 RCMs used in the *PRUDENCE* project assumed SRES A2 and B2 emission scenarios, in contrast to SRES A1B assumed by *ENSEMBLES*. By the end of the century, mean temperature is expected to have increased by between 2·2 and 5·2 °C relative to the average 1980–2009. The increase is more pronounced during the summer months. Changes in annual precipitation are minor (Figure 5B). On average over the catchments, annual precipitation is projected to decrease at a rate of about 9 mm per decade, which is slightly less than the 15 mm per decade estimated by Frei (2007). As for temperature, changes are more pronounced during the summer months. Slight differences occur between the catchments, with regions more exposed to Mediterranean advection (i.e. MTM, GOR, FIN and GRS) becoming dryer than inner-alpine ones.

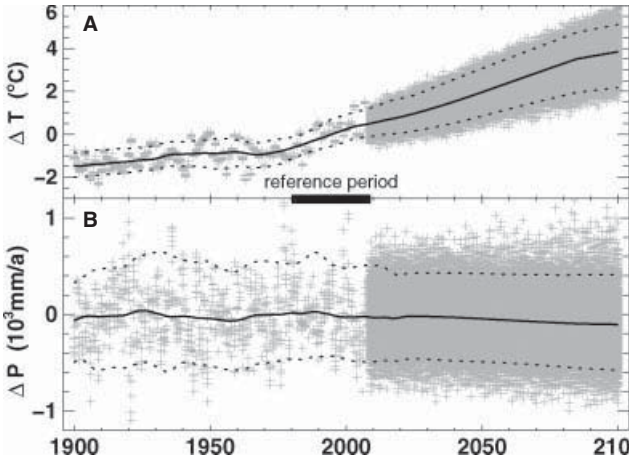

Figure 5. Evolution of mean annual (a) air temperature (T) and (b) annual precipitation sum (P) according to the climate scenarios. The deviation from the mean of the reference period is shown (Δ). All catchments and climate scenarios are shown together (grey crosses). The smoothed median deviation (thick solid line) and a confidence band containing 95% of the data (dotted lines) are displayed. The reference period is marked with the black bar. Smoothing is performed as a 30-year moving average

RESULTS

Runoff evolution

Figure 6 shows the evolution of runoff, evapotranspiration, precipitation, glacierization and the contribution of ice- and snowmelt to total runoff for the modelling period (1900–2100). For runoff, a general pattern, with an initial phase of increased annual discharge, followed by a phase in which discharge decreases, is recognizable for all catchments. However, the magnitude and the timing of the transition differ from basin to basin. The transition is influenced mainly by the degree of glacierization of the catchment, the total ice volume present today and the distribution of glacier ice with altitude. Highly glacierized catchments with a large total ice volume, such as ALE or GOR, show a very pronounced transition, whereas for

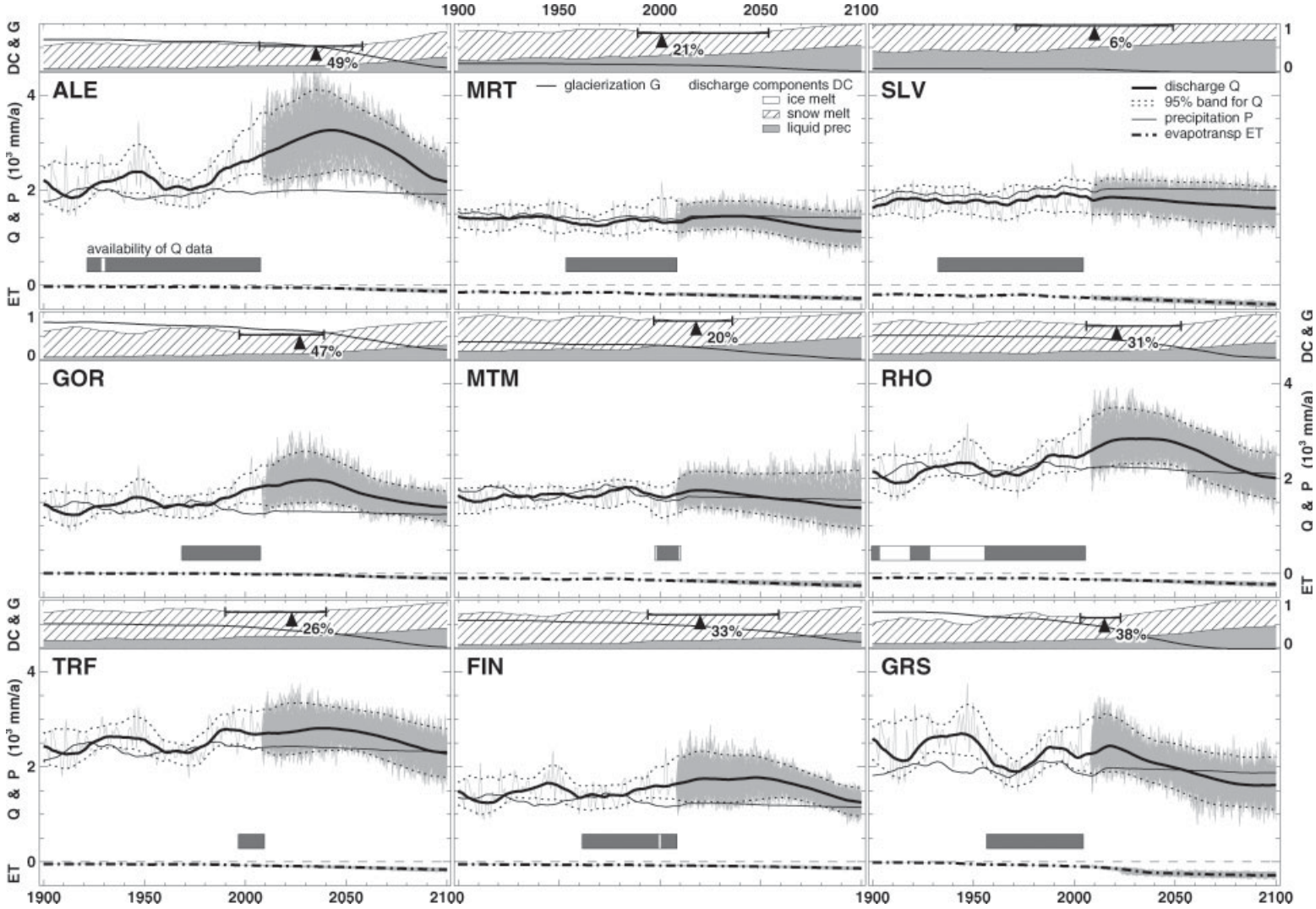

Figure 6. Evolution of annual discharge (Q), precipitation (P), evapotranspiration (ET), discharge components (DC), glacierization (G) and availability of Q data in the different basins. For Q, the trajectories of all individual model realizations (grey lines), a smoothed confidence interval containing 95% of the data (dotted band) and the smoothed median of all realizations (thick black line) is shown. For P, only the smoothed median is shown (thin black line). ET is shown on the same scale as P and Q, but with negative sign (thick dash-dotted line). The dark-grey bar displays the period in which measured data for Q are available. The mean relative contribution of individual DCs to total discharge is displayed on the top panel. The time at which icemelt has the most important contribution is marked with a triangle. The bar around the triangle shows the time span in which the contribution does not vary significantly. The solid line in the same panel shows the glacierized area fraction. Smoothing is performed as a 30-year moving average

basins with small glacierization, such as SLV and MRT, the transition is hardly visible. Depending on the considered catchment, the period in which icemelt (i.e. the runoff generated by the melting of ice) makes the most important contribution to annual discharge is between 2000–2025 (GRS) and 2010–2060 (ALE). The maximal contribution varies between 49 (ALE) and 6% (SLV) and is directly related to the glacierization of the catchment. In relative terms, the contribution of snowmelt (i.e. the runoff generated by the melting of snow) to annual runoff is expected to vary only slightly (−3% on average). This is in line with the results obtained by Weber and others (2010), who analysed the evolution of discharge components in glacierized watersheds of the Austrian Alps. In absolute terms, however, the decrease in annual snowmelt is significant for all catchments, which is in line with the expected shortening of the snow-cover season and the expected increase in the contribution of liquid precipitation. While only 13 to 33% of annual precipitation occurred in liquid form during the reference period, the fraction is expected to increase from 28 to 67% by 2100.

The decreased contribution of snow- and icemelt to total discharge will have a significant influence on the runoff regime, i.e. on the distribution of runoff over the course of the year. In order to characterize these changes, we analyse the temporal evolution of selected quantiles (i.e. 5, 25, 50, 75 and 95% quantiles) of yearly discharge (Figure 7). Significant changes are found for all basins in all of the considered quantiles. The most pronounced changes are found in the outer quantiles (i.e. 5 and 95%), which is an expression of increased runoff during periods of the year which currently show a very low contribution (i.e. the winter months). The magnitude of the changes is catchment-dependent. Basins in which the degree of glacierization is expected to vary most show the most pronounced changes. For GRS, for example, the first 5% of annual discharge are projected to occur about 90 ± 15 days earlier by the end of the century as compared to the reference period. Basins showing less pronounced variations in glacierization show minor variation in the 5% quantile as well. For ALE, the change is in the order of -30 ± 15 days. Besides GRS and SLV, which are expected to be almost ice-free by the end of the century, the contribution of the winter months (December, January and February) to yearly runoff will remain insignificant until 2100. The changes in the central quantiles, in particular the median, are less pronounced. On average over all basins, the day on which 50% of annual runoff occurred is expected to occur earlier at a rate of $2{\cdot}4 \pm 1{\cdot}0$ days per decade. This can be attributed to the earlier onset of the melting season. The day on which the maximal discharge occurs is shifting at a higher rate than the median does. On average, maximal discharge is expected to occur earlier at a rate of $3{\cdot}9 \pm 1{\cdot}7$ days per decade. This indicates that the distribution of the runoff over the year is becoming asymmetric, as expected for the transition from glacial and glacio-nival regime types to nival ones.

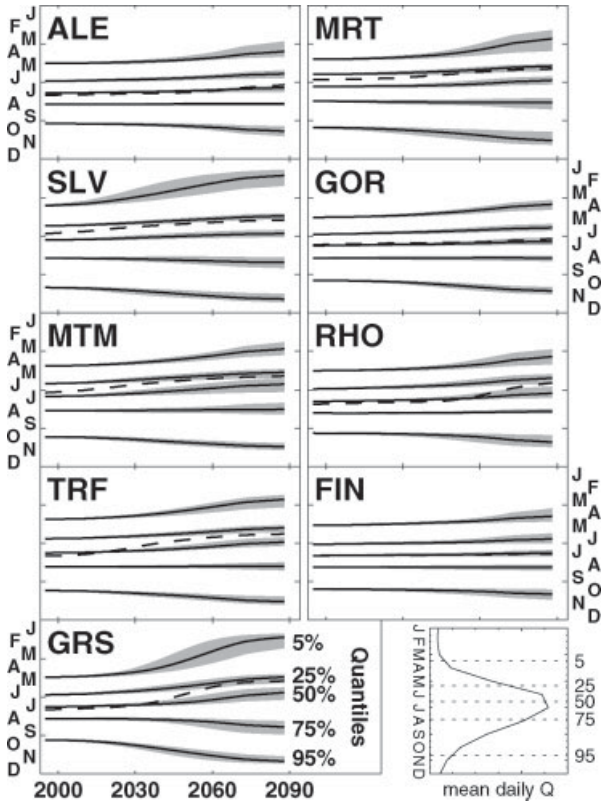

Figure 7. Evolution of runoff regime in the different basins. The temporal evolution of five selected quantiles (5, 15, 50 ,75 and 95%) of the regime curve is shown (solid lines). Grey bands represent 95% confidence intervals. The temporal evolution of maximal discharge (dashed line) is shown without confidence band. The panel in the lower right corner illustrates the concept of quantiles for an imaginary basin with a perfect 'glacio-nival' regime type: the vertical axis corresponds to a one-year period (the letters indicate the 12 months of the year); the horizontal axis displays the mean daily discharge Q of the runoff regime (solid line). At the time labelled '5', 5% of the annual discharge has occurred. In the example, the time corresponds to the end of March. Runoff regimes are evaluated by building mean daily discharges over 30-year periods, and smoothing the resulting curve with a 30-day moving average

Glacier evolution

The projected rise in mean air temperature is reflected in many glaciological variables of hydrological interest, glacier mass balance and duration of the snow-cover season in particular (Figure 8).

Based on a 5-year running mean, no more positive mass balances are expected to occur after 2030 (Figure 8A). Remaining glaciers are expected to slowly approach a new equilibrium state, but this is not projected to happen until the end of the century. Positive mass balances are not expected to occur before 2090. The most negative mass balances are projected for the period 2050–2070, for which mass balance is estimated to be as low as -2 m a^{-1} on a regular basis. This is a level similar to the one experienced in the extraordinary year 2003 (Zemp and others, 2009; Farinotti and others, 2009a), which had considerable effects on the hydrology of glacierized catchments (e.g. Koboltschnig and others, 2009).

The duration of the snow-cover season reflects the evolution of mean annual temperature and is expected to shorten significantly. As a proxy, we considered the

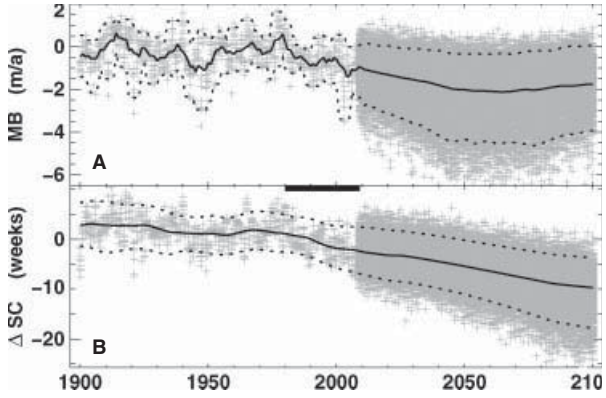

Figure 8. Evolution of (A) annual mass balance (MB) and (B) duration of the snow-cover season (SC). For SC (exact definition in the text), the difference Δ to the reference period (marked with the black band) is shown. Individual data points (grey crosses) are yearly values. The smoothed median (solid line) and a confidence band containing 95% of the data (dotted lines) are displayed. Smoothing is performed as a 5- and 30-year running mean for MB and Δ SC, respectively

number of days in which the snow-covered fraction of the catchment is higher than the average for the reference period. In our simulations, this measure decreases at a rate of 7·5 days per decade and is significant after 2050 (Figure 8B). By the end of the century, the length of the snow-cover season is predicted to have shortened by between 1 and 4 months.

The modelled evolution of the Equilibrium Line Altitude (ELA)—i.e., the glacier elevation for which the annual mass balance is 0—reflects the evolution of mean annual temperature. During the reference period, the ELA averaged over the catchments was at about 3100 m asl, ranging from 2750 m for SLV to about 3350 m for GOR, FIN and MTM. On average, the ELA is projected to increase at a rate of 70 m per decade, leading to an ELA close to the maximal surface elevation for most of the catchments by the end of the century. In all scenarios, the increase in ELA is significant after 2040.

General statements about the evolution of glacier ice volume are difficult to make since the evolution strongly depends on the present glacier state—especially size. Even the most optimistic scenarios however, predict that Grosser Aletschgletscher will lose more than 60% of its present volume by the end of the century. The most pessimistic scenarios predict a complete disappearance of the glacier by the mid-2090s. For small glaciers such as Gries- or Silvrettagletscher, half of the present volume is expected to be lost before 2035. For comparison: between the middle of the reference period (1995) and today (2010), the two glaciers lost about 15 to 20% of their volume.

Specific runoff characteristics related to glacierization

The effect of glaciers on the streamflow of a given basin is well documented in the literature (e.g. Meier and Tangborn, 1961; Stenborg, 1970; Fountain and Tangborn, 1985; Chen and Ohmura, 1990; Pellicciotti and others, 2010). Hock and others (2005) pointed out five specific responses of runoff characteristics to changes in

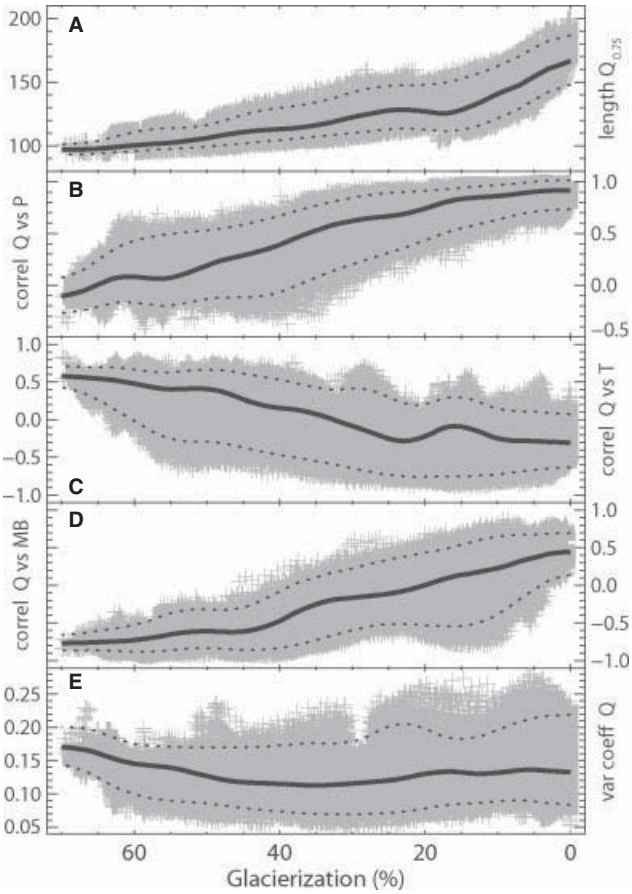

Figure 9. Influence of glacierization on yearly runoff. Glacierization is plotted against (A) length of the period during which 3/4 of the yearly runoff occurs, (B) correlation between annual runoff Q_{yr} and precipitation, (C) correlation between Q_{yr} and mean air temperature, (D) correlation between Q_{yr} and annual mass balance, and (E) coefficient of variation of Q_{yr}. The data from all catchments and all realizations are shown (grey crosses) together with the median (solid line) and a confidence band containing 95% of the data (dashed). Correlations are quantified with Pearson's product-moment correlation coefficient considering 30-year periods. The coefficient of variation is computed for intervals of the same length. A decreasing scale for glacierization is shown as it reflects temporal evolution

the glacierization of a catchment. In the following and in Figure 9A to E, these responses are analysed quantitatively. The model results of the nine catchment and the whole modelling period, i.e. 1900 to 2100, were analysed together. This allows continuous information to be obtained for glacierizations varying between 0 and 70%.

In catchments with a high degree of glacierization, yearly runoff is concentrated during a short period when melt occurs. Figure 9A analyses the length of the period between the 0·125 and the 0·875 quantiles of annual runoff, i.e. the length of the period in which 75% of annual runoff occurs. At glacierizations larger than 50%, three quarters of the yearly runoff occurs during a period shorter than 115 days. At glacierizations of less than 15%, the same runoff fraction occurs in a period longer than that. For glacierizations in between, the period during which 75% of the yearly runoff occur does not change significantly in length and lasts between 100 and 155 days.

In catchments with glacierization of less than 40%, yearly runoff correlates positively with precipitation (Figure 9B). The correlation becomes stronger as the degree of glacierization decreases. In catchments with a glacierization between 40 and 70%, the correlation between precipitation and yearly runoff is not significant. At higher degrees of glacierization, a negative correlation is found. The data basis for this statement is, however, poor.

Although for glacierized catchments a positive correlation between yearly mean temperature and yearly runoff seems intuitive, a significant correlation can only be found at (very) high degrees of glacierization (60% and higher, Figure 9C). For catchments with a degree of glacierization lower than that, the relation shows a large scatter and is not significant. The correlation is obviously more pronounced during the summer period. In this case, significance is found for glacierizations larger than 35% (not shown). These observations can be explained by the fact that even at high degrees of glacierization, precipitation largely contributes to runoff generation.

At glacierizations between 5 and 35%, the yearly runoff does not correlate significantly with the glacier mass balance (Figure 9D). At higher degrees of glacierization, the correlation is negative, meaning that runoff increases in years with negative mass balances. At lower degrees of glacierization, the correlation is positive. The negative correlation between yearly runoff and mass balance at high degrees of glacierization is intuitive, as glaciers strongly contribute to runoff in years of pronounced negative mass balance through meltwater generation. The positive correlation at very low degrees of glacierization can be explained by the fact, that in this case, positive mass balances occur in years with high precipitation sums, i.e. in years when precipitation causes high runoff.

The year-to-year variability of runoff is expected to be smallest at moderate percentages of glacierization, and to increase as glacierization either increases or decreases (Lang, 1987). The statement holds true for each catchment individually, but cannot be generalized in a quantitative manner. In fact, no significant difference is found for the coefficient of variation for glacierizations between 80 and 0% when all catchments are considered together (Figure 9E). Apparently the magnitude of the variability is not steered by the degree of glacierization alone.

DISCUSSION

So far, the bandwidths presented for future runoff reflect the uncertainty of climate evolution only. At least two other sources of uncertainty need to be addressed: the uncertainty in the calibrated parameter set, and the uncertainty in the model itself. All analyses presented so far are performed assuming constant parameters, i.e. parameters which remain unaltered throughout the modelling period. This choice may be questionable, as parameters, especially those steering ablation, may change over different time scales (e.g Braithwaite, 1995; Hock, 2005; Huss, 2009). However, assessing the appropriateness of time-varying parameters is difficult and, thus, a constant parameter set is often the only practicable assumption for simulations extending into the future. By analysing long-term time series of mass balance measurements at stakes, Huss and others (2009) pointed out that the observed variations in the parameters governing the melt model may be linked to a change in the incoming solar radiation. This suggests that semi-empirical approaches, partly capturing the governing physical processes, as well as physical ones, are better suited than merely empirical approaches since parameter variations may be linked to specific processes. However, even for these kinds of approaches, suitable predictions of the parameter evolution do not yet exist.

In order to assess the uncertainty introduced through the calibrated model parameters, we performed a sensitivity analysis based on a so-called 3^k *factorial design* (e.g. Keppel, 1973). That is a Monte Carlo-type experiment (e.g. Hammersley and Handscomb, 1975) with 3^k model runs in which each of the k model parameter is varied over three levels. In our experiment the mean level corresponds to the previously calibrated parameter value and the upper and the lower level are chosen by varying the mean level by $\pm 50\%$. The experiment is performed only for MTM—which has the median size of the considered catchments and includes all represented surface types—and only for the reference period 1980–2009. In the analysis, we focus on the parameters affecting annual discharge. Parameters which steer the discharge on sub yearly time scales (i.e. all parameters of the runoff routing module beside the retention constant of the slow reservoir) are left unaltered. Since the magnitude of annual evapotranspiration during the reference period is not significant for all considered catchments, we leave the parameters of this module unaltered as well. This results in a 3^8 experiment—i.e. a total of 6561 model runs—in which we vary three parameters of the ablation module (f_M, r_{ice} and r_{snow}, Equation 2), two parameters of the accumulation module (c_{prec} and dP/dz, Equation 1), the temperature lapse rate (dT/dz) and the two parameters controlling the runoff from the slow reservoir (V_{slow_max} and k_{slow}, Equations 5 and 6).

The data generated in the described experiment are evaluated by setting up two multiple linear regression (MLR) models: (1) in the first one, the explanatory variables are the relative variation of the considered parameters (including two-way interactions) and the target variable is the relative difference in mean annual discharge compared to the reference run (i.e. the run with the unaltered, calibrated parameters); (2) in the second regression model, the same explanatory variables are used, but the target variable is defined as the logarithm of the difference between the sum-of-squares (SSQ) of the residuals given by the modelled and the measured daily discharge. The sum is performed over the period in which measured discharge is available and the logarithm

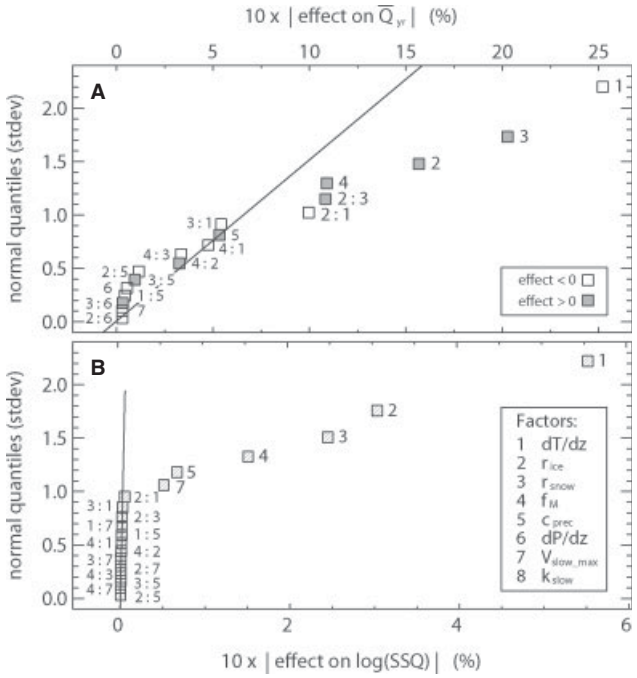

Figure 10. Assessment of sensitivity and robustness of the parameters (factors) of *GERM*. Half-normal plots for the multiple linear regression (MLR) analysis performed in the MTM basin with (A) mean annual discharge $\overline{Q}_{yr}$ and (B) logarithm of the sum-of-squares *log(SSQ)* as target variables are shown. 'M : N' denotes a first order interaction between the factors M and N. All displayed factors are significant at a 5% level in the MLR model reduced by backward selection. 'Important' factors clearly depart from the solid line, i.e. the line passing through the origin and having slope *median(Y)/median(X)*, where *X* and *Y* are the abscissa and the ordinate of the data points, respectively

is taken as the difference in *SSQ* to the reference run is always non-negative (Mosteller and Tukey, 1977, call this a 'first-aid transformation'). The first analysis allows the sensitivity of total discharge to be assessed with respect to the parameters, the second one gives an indication on the robustness of the chosen parameters.

Figure 10A and B show the half-normal probability plots (Daniel, 1959) for the explanatory variables which are significant in the two analyses after having reduced the MLR models through backward selection—that is by omitting the non-significant variables one by one until all those remaining are significant at a 5% level (e.g. Draper and others, 1998). In the plot, 'important' variables clearly depart from the solid line.

The mean annual discharge $\overline{Q}_{yr}$ (Figure 10A) is affected mostly by the temperature gradient dT/dz: an increase of 10% in dT/dz, reduces $\overline{Q}_{yr}$ by about 25%. This is because temperature controls both the phase of precipitation and the melt rates of snow and ice. For high elevations of the basin, a reduction of dT/dz implies a higher temperature, which enhances melt and reduces accumulation, both increasing $\overline{Q}_{yr}$. The three parameters of the ablation model—f_M, r_{ice} and r_{snow}—play an important role as well: an increase of 10% in one of the parameters, rises $\overline{Q}_{yr}$ by 11, 16 and 20%, respectively. Note the relevance of the interactions between r_{ice} and r_{snow}, as well as between r_{ice} and dT/dz. An interaction means that the effect of the variation of a single parameter is dependent on the level of the other parameters. For example: if r_{snow} is left at the reference level, an increase of 10% in r_{ice} increases $\overline{Q}_{yr}$ by 16%—as stated above—however, if r_{snow} is 10% higher than in the reference case, an increase of 10% in r_{ice} increases $\overline{Q}_{yr}$ by 27% (16% from the main effect + 11% from the interaction). The effects of the other parameters—in particular those of the accumulation module—can be considered to have minor relevance and are not further discussed.

When considering the effects of the parameters on *SSQ* (Figure 10B), the importance of the interactions almost vanishes, although 13 out of the 28 possible two-way interactions remain significant at a 5% level. This means that the effect of the variation of any parameter remains unaltered regardless of the value assigned to the other variables. Note that log(*SSQ*) increases for both, an increase or a decrease in any of the parameters. The analysis points out again the importance of dT/dz: a variation of 10% in dT/dz increases *log(SSQ)* by 5·5%. The parameters of the ablation module play an important role as well: a variation of 10% in f_M, r_{ice} or r_{snow}, causes *SSQ* to rise by 1·5, 2·5 and 3·0%, respectively.

Considering the results of the sensitivity and robustness analyses, the first parameter which should be assessed in respect to its temporal stability is the temperature lapse rate. The sensitivity of temperature-index melt models to the temperature lapse rate was already reported (e.g. Gardner and Sharp, 2009), and yet, although the seasonality of the variable is well documented (e.g. Rolland, 2003; Blandford and others, 2008), the variability on a longer time scale has seldom been addressed. Gardner and Sharp (2009) suggested that in a warming climate, lower near-surface temperature lapse rates can be expected, but there is no consensus about this statement. Generally, climate models do not provide an explicit scenario for the evolution of the temperature lapse rate and implicit projections, derivable for example from scenarios for locations at different elevations, are not considered to be reliable. The assumption of constant lapse rates is, thus, the only practicable method for long-term projections.

As shown, the parameters of the melt module also have to be considered sensitive, and deserve attention regarding their potential changes in time. In addition to the already mentioned possible variations in the energy balance components, processes such as the albedo-lowering of the ice surfaces due to dust and black carbon deposition and reduced winter accumulation may change the empirical relations upon which temperature-index approaches are based. Different authors pointed out that this kind of process may play a significant role in the future (e.g. Paul and others, 2006; Oerlemans and others, 2009).

The fact that in the sensitivity analysis some interaction remains significant suggests that some combinations of parameters are not particularly well defined, i.e. that similar results could be obtained also by choosing a different parameter combination. This is known as the 'problem of equifinality' (e.g. Beven, 2006). In this regard, one has

to note that our experiment analysed the sensitivity of the parameters with respect to discharge only, and it is thus not surprising that the interaction between r_{ice} and r_{snow}, for instance, is significant (the same discharge can be obtained by melting much snow and little ice or vice versa). However, the problem persists to some degree. In fact, even if we take different types of data into account for our calibration, which is known to improve significantly the internal model consistency (e.g. Schäfli and Huss, 2010; Finger and others, 2011), we cannot exclude that the values calibrated for some parameters may compensate the effect of certain others. This complicates the intercomparison of parameters calibrated for individual catchments and we therefore do not interpret any pattern which may be visible in the values stated in Table III.

Finally, the uncertainty related to the model itself has to be addressed. Uhlenbrook and Leibundgut (2002) call this the 'model-structure uncertainty'. Although each module within *GERM* has been shown to perform well when calibrated accurately, 'structural uncertainties' are introduced at each modelling step: the accumulation module parametrizes spatial variations in a simple, descriptive, manner, neglecting the underlying processes; the ablation and evapotranspiration modules are based on statistical relations, which reflect the governing physical processes only in part; the glacier evolution module is empirical and does not include any mechanical or thermodynamical principles, and the runoff routing module is based on the concept of linear reservoirs, which is only a crude representation of nature. And even the meteorological time series required as input are associated with uncertainties relating to the methods from which they are derived.

For the assessment of the model-structure uncertainty, some valid approaches, based for instance on state-space filtering methods such as the ensemble Kalman filter (Evensen, 1994), or on Bayesian model-averaging techniques (e.g. Hoeting and others, 1999) have been presented (e.g. Moradkhani and others, 2005; Vrugt and others, 2005; Ajami and others, 2007). However, these kind of techniques are still not state-of-the-art in hydrology and in many other fields of research. Ensemble runs, as used for the realisation of the climate scenarios applied, are rather uncommon in most modelling studies. The reason for this is often the large amount of computational resources required for such experiments (Ajami and others, 2007). This limitation affects the present contribution as well.

When aiming at providing projections for long-term evolutions, the uncertainty linked to the model choice may play a significant role. In various fields of natural sciences, physically-based models have gradually become more popular since it is suggested that such models are better suited for projections in an environment with changing boundary conditions as the climate. In hydrology, examples of established physically-based models are *MIKE-SHE* (Refsgaard and Strom, 1996) or *WASIM-ETH* (Schulla, 1997). However, conceptual models based on statistical relations obtained from past observations retain their importance for forecast analyses. Models such as *TOPMODEL* (Beven and Kirkby, 1979), *PRMS* (Leavesley and others, 1983), *HBV* (Bergström, 1995) or *TOPKAPI* (Ciarapica and Todini, 2002), have been shown to perform well in this respect. *GERM* is a model which fits well into this class. Obviously, a comprehensive assessment of the uncertainties of such models is equally important as the assessment of the bandwidth and the uncertainties of climate scenarios.

CONCLUSIONS

In this contribution we presented hydrological and glaciological projections for nine high-alpine catchments in the Swiss Alps with widespread morphological characteristics. The main focus of the analyses was the assessment of the uncertainties introduced by the unknown climate evolution. We used a conceptual model composed of individual modules based on statistical relationships derived from data in the past. The results were presented in order to highlight common characteristics between catchments and were formulated in a general way, in order to remain valid for other comparable, high-alpine basins.

According to our results it can be stated that:

1. By the end of the century, mean air temperature is expected to have increased between 2·2 and 5·2 °C relative to the reference period 1980–2009. This corresponds to an average rate of $+0{\cdot}4 \pm 0{\cdot}1$ °C per decade.
2. Changes in annual precipitation are minor and location dependent. Annual precipitation is expected to decrease in the order of 5% in Alpine catchments exposed to Mediterranean advection and to remain almost unaltered in inner-alpine regions.
3. The distribution of runoff over the year will have more pronounced changes in catchments with a high degree of glacierization. A transition from glacial and glacionival regime types to nival ones will occur. The time of year with maximal daily discharges is expected to occur earlier at a rate of $4{\cdot}4 \pm 1{\cdot}7$ days per decade.
4. General statements about absolute variations in discharge are not reliable since the evolution depends strongly on the basin considered. A general pattern, with an initial phase of increased annual discharge, followed by a phase in which discharge decreases, is recognizable for all catchments with a significant degree of glacierization. The timing of maximal annual runoff is projected to occurr before 2050 in all basins.
5. By the end of the century, the fraction of precipitation occurring in liquid form is expected to increase by 15 to 35% compared to the present level. The contribution of snowmelt to annual discharge will decrease accordingly.
6. Yearly runoff correlates positively with annual precipitation in catchments with glacierization of less than 40%. The correlation becomes stronger as glacierization decreases. For glacierizations between 40 and 70%, the correlation is not significant.

7. Glacier mass balance has a significant effect on annual discharge for a degree of glacierization lower than 5% (positive correlation) and higher than 35% (negative correlation).

ACKNOWLEDGEMENTS

This study was funded by the projects *CCHydro* (Swiss Federal Office for the Environment, BAFU), *FUGE* (Swiss National Science Foundation, NFP 61) and *WWK* (Department of Energy and Hydro Power, Canton Valais, and Forces Motrices Valaisannes). The delta-change scenario data were distributed by the Center for Climate Systems Modeling (C2SM). The data were derived from regional climate simulations of the EU FP6 Integrated Project *ENSEMBLES* (Contract number 505539) whose support is gratefully acknowledged. The dataset was prepared by Thomas Bosshard at ETH Zurich, partly funded by swisselectric/Swiss Federal Office of Energy(BFE) and CCHydro/Swiss Federal Office for the Environment (BAFU). H. Bösch and B. Nedela are acknowledged for their support in the preparation of the required DEMs. Runoff data were kindly provided by BAFU, Grand Dixence S.A., Kraftwerke Mattmark A.G., Oberhäsli A.G. and Aegina A.G. S. Braun-Clarke proofread the manuscript. We acknowledge M. Anderson for the editorial work and four anonymous reviewers for their helpful comments.

REFERENCES

Ajami NK, Duan Q, Sorooshian S. 2007. An integrated hydrologic Bayesian multimodel combination framework: confronting input, parameter, and model structural uncertainty. *Water Resources Research* **43**: W01403.

Bauder A, Funk M, Huss M. 2007. Ice volume changes of selected glaciers in the Swiss Alps since the end of the 19th century. *Annals of Glaciology* **46**: 145–149.

Becker A. 2005. Runoff processes in mountain headwater catchments: recent understanding and research challenges. *Advances in Global Change Research* **23**(III): 283–295.

Begert M, Schlegel T, Kirchhofer W. 2005. Homogeneous temperature and precipitation series of Switzerland from 1864 to 2000. *International Journal of Climatology* **25**(1): 65–80.

Bergströom S. 1995. The HBV model. In *Computer Models of Watershed Hydrology*, Singh V (ed). Highlands Ranch: Colorado, USA; 443–476.

Bernath A. 1991. Wasserhaushalt im Einzugsgebiet der Rhône bis Gletsch. Untersuchungen zu Niederschlag, Verdunstung und Abfluss in einem teilweise vergletscherten Einzugsgebiet. *Zürcher Geographische Schriften* **43**: 383 pp.

Beven K. 2006. A manifesto for the equifinality thesis. *Journal of Hydrology* **320**(1–2): 18–36.

Beven HJ, Kirkby MJ. 1979. A physically based, variable contributing area model of basin hydrology. *Hydrological Sciences Bulletin* **24**(1): 43–70.

Blandford TR, Humes KS, Harshburger BJ, Moore BC, Walden VP. 2008. Seasonal and synoptic variations in near-surface air temperature lapse rates in a mountainous basin. *Journal of Applied Meteorology and Climatology* **47**: 249–261.

Bosshard T, Kotlarsky S, Ewen T, Schär C. 2011. Spectral representation of the annual cycle in the climate change signal. *Hydrology and Earth System Sciences Discussion* **8**: 1161–1192.

Braithwaite RJ. 1995. Positive degree-day factors for ablation on the Greenland ice sheet studied by energy-balance modelling. *Journal of Glaciology* **41**(137): 153–160.

Bruce JP, Clark RH. 1981. *Introduction to Hydrometeorology*. Pergamon Press: Oxford.

Chen J, Ohmura A. 1990. On the influence of Alpine glaciers on runoff. In *Hydrology in Mountainous Regions, Proceedings of Two Lausanne Symposia, August 1990*, IAHS Publ. No. 193., Lang H, Musy A (eds). 117–125.

Christensen JH, Carter T, Giorgi F. 2002. PRUDENCE employs new methods to assess European climate change. *EOS* **83**(13): 147.

Christensen JH, Christensen OB. 2007. A summary of the PRUDENCE model projections of changes in European climate by the end of this century. *Climatic Change* **81**: 7–30.

Ciarapica L, Todini E. 2002. TOPKAPI: a model for the representation of the rainfall-runoff process at different scales. *Hydrological Processes* **16**(2): 207–229.

Daniel C. 1959. Use of half-normal plots in interpreting factorial two-level experiments. *Technometrics* **1**: 311–341.

Draper NR, Smith H, Pownell E. 1998. *Applied regression analysis*. Wiley-Interscience: New York.

EEA. 2009. *Regional Climate Change and Adaptation—The Alps Facing the Challenge of Changing Water Resources*. European Environment Agency: Copenhagen, Report Nr. 8.

Engelen G. 2000. MODULUS: a spatial modelling tool for integrated environmental decision-making. Directorate General XII, Environment IV Framework, Brussels, Belgium, Final Report.

Evensen G. 1994. Sequential data assimilation with a nonlinear quasigeostrophic model using Monte Carlo methods to forecast error statistics. *Journal of Geophysical Research* **99**(10): 10143–10162.

Farinotti D. 2010. Simple methods for inferring glacier ice-thickness and snow-accumulation distribution. Ph.D. thesis, ETH Zürich, dissertation No. 19268.

Farinotti D, Huss M, Bauder A, Funk M. 2009a. An estimate of the glacier ice volume in the Swiss Alps. *Global and Planetary Change* **68**: 225–231.

Farinotti D, Huss M, Bauder A, Funk M, Truffer M. 2009b. A method to estimate ice volume and ice thickness distribution of alpine glaciers. *Journal of Glaciology* **55**(191): 422–430.

Finger D, Pellicciotti F, Konz M, Rimkus S, Burlando P. 2011. The value of glacier mass balance, satellite snow cover images and hourly discharge for improving the performance of a physically based distributed hydrological model. *Water Resources Research* **47**: W07519, DOI:10.1029/2010WR009824.

Fountain AG, Tangborn WV. 1985. The effect of glaciers on streamflow variations. *Water Resources Research* **21**(4): 579–586.

Frei C. 2007. Climate Change and Switzerland 2050—Impacts on Environment, Society and Economy, Advisory Body on Climate Change (OcCC), http://www.occc.ch.

Gardner AS, Sharp M. 2009. Sensitivity of net mass-balance estimates to near-surface temperature lapse rates when employing the degree-day method to estimate glacier melt. *Annals of Glaciology* **50**(50): 80–86.

Gremaud V, Goldscheider N. 2010. Climate change effects on aquifer recharge in a glacierised karst aquifer system, Tsanfleuron-Sanetsch, Swiss Alps. In *Advances in Research in Karst Media*, Andreo B Carrasco F, Durán JJ and LaMoreaux JW (eds). Springer, Berlin Heidelberg; 31–36.

Hammersley JM, Handscomb DC. 1975. *Monte Carlo Methods*. Halsted-Press: New York.

Hamon WR. 1961. Estimating potential evapotranspiration. *Journal of the Hydraulics Division* **87**(HY3): 107–120.

Hattermann FF, Post J, Krysanova V, Conradt T, Wechsung F. 2008. Assessment of water availability in a central-European river basin (Elbe) under climate change. *Advances in Climate Change Research* **4**: (Suppl.): 42–50.

Hock R. 1999. A distributed temperature-index ice- and snowmelt model including potential direct solar radiation. *Journal of Glaciology* **45**(149): 101–111.

Hock R. 2005. Glacier melt: a review of processes and their modelling. *Progress in Physical Geography* **29**(3): 362–391.

Hock R, Jansson P, Braun L. 2005. Modelling the response of mountain glacier discharge to climate warming. In *Global Change and Mountain Regions—A State of Knowlegde Overview*, Huber UM, Reasoner MA, Bugmann H (eds). Springer: Dordrecht; 243–252.

Hoeting JA, Madigan D, Raftery AE, Volinsky CT. 1999. Bayesian model averaging: a tutorial. *Statistical Science* **14**(4): 382–417.

Horton P, Schäfli B, Mezghani A, Hingray B, Musy A. 2006. Assessment of climate-change impacts on alpine discharge regimes with climate model uncertainty. *Hydrological Processes* **20**(10): 2091–2109.

Huber UM, Reasoner MA, Bugmann H. 2005. *Global Change and Mountain Regions—A State of Knowlegde Overview*. Springer: Dordrecht.

Huss M, Bauder A, Funk M, Hock R. 2008a. Determination of the seasonal mass balance of four Alpine glaciers since 1865. *Journal of Geophysical Research* **113**: F01015.

Huss M, Farinotti D, Bauder A, Funk M. 2008b. Modelling runoff from highly glacierized alpine catchment basins in a changing climate. *Hydrological Processes* **22**(19): 3888–3902.

Huss M, Bauder A, Funk M. 2009. Homogenization of long-term mass balance time series. *Annals of Glaciology* **50**(50): 198–206.

Huss M, Hock R, Bauder A, Funk M. 2010a. 100-year glacier mass changes in the Swiss Alps linked to the Atlantic Multidecadal Oscillation. *Geophysical Research Letters* **37**: L10501.

Huss M, Jouvet G, Farinotti D, Bauder A. 2010b. Future high-mountain hydrology: a new parameterization of glacier retreat. *Hydrology and Earth System Sciences Discussion* **7**: 345–387.

IPCC. 2000. *IPCC Emission Scenarios (SRES)*, Nakicenovic N, Swart R (eds). Cambridge University Press; 570.

IPCC. 2007. *Climate Change 2007: Contribution of Working Group I to the Fourth Assessment Report of the IPCC*, Technical report, Solomon S, Qin D, Manning M, Chen Z, Marquis M, Averyt KB, Tignor M, Miller HL (eds). Cambridge University Press.

Jasper K, Calanca P, Gyalistras D, Fuhrer J. 2004. Differential impacts of climate change on the hydrology of two alpine river basins. *Climate Research* **26**: 113–129.

de Jong C, Collins D, Ranzi R. 2005. *Climate and Hydrology in Mountain Areas*. Wiley: West Sussex, England.

de Jong C, Lawler D, Essery R. 2009. Mountain hydroclimatology and snow seasonality—perspectives on climate impacts, snow seasonality and hydrological change in mountain environments. *Hydrological Processes* **23**: 955–961.

Jouvet G, Picasso M, Rappaz J, Blatter H. 2008. A new algorithm to simulate the dynamics of a glacier: theory and applications. *Journal of Glaciology* **54**(188): 801–811.

Keppel G. 1973. *Design and analysis—a researcher's handbook*. Prentice-Hall: Englewood Cliffs, NJ.

Kirpich ZP. 1940. Time of concentration of small agricultural watersheds. *Civil Engineering* **10**(6): 362.

Koboltschnig GR, Schöner W, Holzmann H, Zappa M. 2009. Glaciermelt of a small basin contributing to runoff under the extreme climate conditions in the summer of 2003. *Hydrological Processes* **23**(7): 1010–1018.

Lang H. 1987. Forecasting meltwater runoff from snow-covered areas and from glacier basins. In *River Flow Modelling and Forecasting*, Kraijenhoff DA, Moll JR (eds). Reidel: Dordrecht; 99–127.

Lang H, Schädler B, Davidson G. 1977. Hydroglaciological investigations on the Ewigschneefeld-Grosser Aletschgletscher. *Zeitschrift füur Gletscherkunde und Glazialgeologie* **12**: 109–124.

Langbein WB. 1958. Queuing theory and water storage. *Journal of the Hydraulics Division of the U.S.G.S.* **84**(5): 1–24.

Leavesley GH, Lichty RW, Troutman B, Saindon LG. 1983. Precipitation-runoff modelling system. User's manual. Technical report, USGS Water Resources Investigations, report 83-4238.

Liniger H, Weingartner R, Grosjean M. 1998. Mountains of the world—Water towers for the 21st century, Centre for Development and Environment, Berne, Switzerland. Prepared by Mountain Agenda for the Commission on Sustainable Development (CSD).

Ludwig R, Mauser W, Niemeyer S, Colgan A, Stolz R, Escher-Vetter H, Kuhn M, Reichstein M, Tenhunen J, Kraus A, Ludwig M, Barth M, Hennicker R. 2003. Web-based modelling of energy, water and matter fluxes to support decision making in mesoscale catchments—the integrative perspective of GLOWA-Danube. *Physics and Chemistry of the Earth* **28**: 621–634.

Mauser W, Bach H. 2009. PROMET—large scale distributed hydrological modelling to study the impact of climate change on the water flows of mountain watersheds. *Journal of Hydrology* **376**(3–4): 362–377.

Meier MF, Tangborn WV. 1961. Distinctive characteristics of glacier runoff. *U.S. Geological Survey Professional Paper* **424-B**: 14–16.

Mesinger F, Pierrehumbert RT. 1986. Alpine lee cyclogenesis: numerical simulation and theory, scientific results of the alpine experiment (ALPEX). Volume I, GARP Publication Series, 141–163, no. 27.

Moradkhani H, Sorooshian S, Gupta HV, Hauser PR. 2005. Dual state-parameter estimation of hydrological models using ensemble Kalman filter. *Advances in Water Resources* **28**: 135–147.

Mosteller F, Tukey JW. 1977. *Data analysis and regression: a second course in statistics*. Addison-Wesley: Reading, MA.

Nash JE, Sutcliffe JE. 1970. River flow forecasting through conceptual models, Part I: a discussion of principles. *Journal of Hydrology* **10**: 282–290.

Oerlemans J, Giessen R, van den Broeke M. 2009. Retreating alpine glaciers: increased melt rates due to accumulation of dust (Vadret da Morteratsch, Switzerland). *Journal of Glaciology* **55**(192): 729–761.

Paul F, Kääb A, Haeberli W. 2006. Recent glacier changes in the Alps observed by satellite: consequences for future monitoring strategies. *Global and Planetary Change* **56**(1–2): 111–122.

Peck EL, Brown MJ. 1962. An approach to the development of isohyetal maps for mountainous areas. *Journal of Geophysical Research* **67**: 681–694.

Pellicciotti F, Bauder A, Parola M. 2010. Effect of glaciers on streamflow trends in the Swiss Alps. *Water Resources Research* **46**: W10522.

Refsgaard JC, Storm B. 1996. Construction, calibration and validation of hydrological models. In *Distributed Hydrological Modelling*, Abbott MB, Refsgaard JC (eds). Kluwer Academic: Dordrecht, Netherlands; 41–54.

Rolland C. 2003. Spatial and seasonal variations of air temperature lapse rates in Alpine regions. *Journal of Climate* **16**: 1032–1046.

Romerio F. 2008a. Hydroelectric resources between State and Market in the Alpine countries. In *Mountains: Sources of water, Sources of knowledge*, *Vol. 31 of Advances in Global Change Research*, Wiegandt Ellen (ed). Springer: New York; 83–99.

Romerio F. 2008b. Regional policy and hydroelectric resources. *Journal of Alpine Research* **96**(1): 79–89.

Schädler B, Weingartner R. 2010. Impact of climate change on water resources in the Alpine regions of Switzerland. In *Alpine Waters*, Bundi U (ed). Springer-Verlag: Berlin Heidelberg; 59–69.

Schäfli B, Hingray B, Niggli M, Musy A. 2005. A conceptual glacio-hydrological model for high mountainous catchments. *Hydrology and Earth System Sciences* **9**: 95–109.

Schäfli B, Hingray B, Musy A. 2007. Climate change and hydropower production in the Swiss Alps: quantification of potential impacts and related modelling uncertainties. *Hydrology and Earth System Sciences* **11**(3): 1191–1205.

Schäfli B, Huss M. 2010. Simulation of high mountainous discharge: how much information do we need? *Hydrology and Earth System Sciences Discussion* **7**: 8661–8702.

Schulla J. 1997. Hydrological modeling of river basins to evaluate the impact of climate change. *Züricher Geographische Hefte* **65**: ETH Zurich, Switzerland.

Schwarb M, Daly C, Frei C, Schär C. 2001. Mean annual and seasonal precipitation throughout the European Alps 1971-1990. Technical report, Hydrological Atlas of Switzerland, plates 2.6, 2.7.

Stahl K, Moore RD, Shea JM, Hutchinson D, Cannon AJ. 2008. Coupled modelling of glacier and streamflow response to future climate scenarios. *Water Resources Research* **44**: W02422.

Stenborg T. 1970. Delay of run-off from a glacier basin. *Geografiska Annaler* **52A**: 1–30.

Stewart IT. 2009. Changes in snowpack and snowmelt runoff for key mountain regions. *Hydrological Processes* **23**: 78–94.

Tarboton DG, Chowdhury TG, Jackson TH. 1995. A spatially distributed energy balance snowmelt model. In Biogeochemistry of Seasonally Snow-Covered Catchments, Proceedings of a Boulder Symposium, IAHS Publ. No. 228, Tonnessen KA, Williams MW, Tranter M (eds). 141–155.

Uhlenbrook S, Leibundgut Ch. 2002. Process-oriented catchment modelling and multiple-response validation. *Hydrological Processes* **16**: 423–440.

van der Linden P, Mitchell JFB. 2009. *ENSEMBLES: Climate Change and Its Impacts: Summary of Research and Results From the ENSEMBLES Project*. Met Office Hadley Centre: UK; 160.

Verbunt M, Gurtz J, Jasper K, Lang H, Warmerdam P, Zappa M. 2003. The hydrological role of snow and glaciers in alpine river basins and their distributed modeling. *Journal of Hydrology* **282**(1–4): 36–55.

Viviroli D, Dürr HH, Messerli B, Meybeck M. 2007. Mountains of the world, water towers for humanity: typology, mapping, and global significance. *Water Resources Research* **43**: W07447.

Viviroli D, Archer DR, Buytaert W, Fowler HJ, Greenwood GB, Hamlet AF, Huang Y, Koboltschnig G, Litaor MI, López-Moreno JI, Lorentz S, Schädler B, Schwaiger K, Vuilleand M, Woods R. 2011. Climate change and mountain water resources: overview and recommendations for research, management and politics. *Hydrology and Earth System Sciences Discussion* **7**: 2829–2895.

Vrugt JA, Diks CGH, Gupta HV, Bouten W, Verstraten JM. 2005. Improved treatment of uncertainty in hydrologic modeling: combining the strengths of global optimization and data assimilation. *Water Resources Research* **41**: W01017.

Wallén, C. C., ed., 1970. *Climates of Northern and Western Europe, World Survey of Climatology*, Vol. 5 and 6, Elsevier Scientific Publishing Company: Amsterdam.

Weber M, Braun L, Mauser W, Prasch M. 2010. Contribution of rain, snow- and icemelt in the upper Danube discharge today and in the future. *Geografia Fisica e Dinamica Quaternaria* **33**: 221–230.

Zemp M, Hoelzle M, Haeberli W. 2009. Six decades of glacier mass-balance observations: a review of the worldwide monitoring network. *Annals of Glaciology* **50**(50): 101–111.